












04-06

April 2006



TECH BRIEFS

NATIONAL AERONAUTICS AND SPACE ADMINISTRATION

-  **Technology Focus**
-  **Electronics/Computers**
-  **Software**
-  **Materials**
-  **Mechanics**
-  **Machinery/Automation**
-  **Manufacturing & Prototyping**
-  **Bio-Medical**
-  **Physical Sciences**
-  **Information Sciences**
-  **Books and Reports**

INTRODUCTION

Tech Briefs are short announcements of innovations originating from research and development activities of the National Aeronautics and Space Administration. They emphasize information considered likely to be transferable across industrial, regional, or disciplinary lines and are issued to encourage commercial application.

Availability of NASA Tech Briefs and TSPs

Requests for individual Tech Briefs or for Technical Support Packages (TSPs) announced herein should be addressed to

National Technology Transfer Center

Telephone No. (800) 678-6882 or via World Wide Web at www2.nttc.edu/leads/

Please reference the control numbers appearing at the end of each Tech Brief. Information on NASA's Innovative Partnerships Program (IPP), its documents, and services is also available at the same facility or on the World Wide Web at <http://ipp.nasa.gov>.

Innovative Partnerships Offices are located at NASA field centers to provide technology-transfer access to industrial users. Inquiries can be made by contacting NASA field centers and Mission Directorates listed below.

NASA Field Centers and Program Offices

Ames Research Center

Lisa L. Lockyer
(650) 604-1754
lisa.l.lockyer@nasa.gov

Dryden Flight Research Center

Gregory Poteat
(661) 276-3872
greg.poteat@dfrc.nasa.gov

Goddard Space Flight Center

Nona Cheeks
(301) 286-5810
Nona.K.Cheeks.1@nasa.gov

Jet Propulsion Laboratory

Ken Wolfenbarger
(818) 354-3821
james.k.wolfenbarger@jpl.nasa.gov

Johnson Space Center

Helen Lane
(713) 483-7165
helen.w.lane@nasa.gov

Kennedy Space Center

Jim Aliberti
(321) 867-6224
Jim.Aliberti-1@nasa.gov

Langley Research Center

Ray P. Turcotte
(757) 864-8881
r.p.turcotte@larc.nasa.gov

John H. Glenn Research Center at Lewis Field

Robert Lawrence
(216) 433-2921
robert.f.lawrence@nasa.gov

Marshall Space Flight Center

Vernotto McMillan
(256) 544-2615
vernotto.mcmillan@msfc.nasa.gov

Stennis Space Center

John Bailey
(228) 688-1660
john.w.bailey@nasa.gov

NASA Mission Directorates

At NASA Headquarters there are four Mission Directorates under which there are seven major program offices that develop and oversee technology projects of potential interest to industry:

Carl Ray

Small Business Innovation Research Program (SBIR) & Small Business Technology Transfer Program (STTR)
(202) 358-4652
carl.g.ray@nasa.gov

Frank Schowengerdt

Innovative Partnerships Program (Code TD)
(202) 358-2560
fschowen@hq.nasa.gov

John Mankins

Exploration Systems Research and Technology Division
(202) 358-4659
john.c.mankins@nasa.gov

Terry Hertz

Aeronautics and Space Mission Directorate
(202) 358-4636
thertz@mail.hq.nasa.gov

Glen Mucklow

Mission and Systems Management Division (SMD)
(202) 358-2235
gmucklow@mail.hq.nasa.gov

Granville Paules

Mission and Systems Management Division (SMD)
(202) 358-0706
gpaules@mtpe.hq.nasa.gov

Gene Trinh

Human Systems Research and Technology Division (ESMD)
(202) 358-1490
eugene.h.trinh@nasa.gov

John Rush

Space Communications Office (SOMD)
(202) 358-4819
john.j.rush@nasa.gov



TECH BRIEFS

NATIONAL AERONAUTICS AND SPACE ADMINISTRATION



5 Technology Focus: Sensors

- 5 Replaceable Sensor System for Bioreactor Monitoring
- 5 Unitary Shaft-Angle and Shaft-Speed Sensor Assemblies
- 6 Arrays of Nano Tunnel Junctions as Infrared Image Sensors
- 7 Catalytic-Metal/PdO_x/SiC Schottky-Diode Gas Sensors
- 8 Compact, Precise Inertial Rotation Sensors for Spacecraft



9 Electronics/Computers

- 9 Universal Controller for Spacecraft Mechanisms
- 9 The Flostation — an Immersive Cyberspace System
- 10 Algorithm for Aligning an Array of Receiving Radio Antennas
- 11 Single-Chip T/R Module for 1.2 GHz



13 Software

- 13 Quantum Entanglement Molecular Absorption Spectrum Simulator
- 13 FuzzObserver
- 13 Internet Distribution of Spacecraft Telemetry Data
- 13 Semi-Automated Identification of Rocks in Images

- 14 Pattern-Recognition Algorithm for Locking Laser Frequency



15 Materials

- 15 Designing Cure Cycles for Matrix/Fiber Composite Parts



17 Machinery/Automation

- 17 Controlling Herds of Cooperative Robots
- 17 Modification of a Limbed Robot to Favor Climbing



19 Bio-Medical

- 19 Vacuum-Assisted, Constant-Force Exercise Device
- 20 Production of Tuber-Inducing Factor



21 Physical Sciences

- 21 Quantum-Dot Laser for Wavelengths of 1.8 to 2.3 μm
- 21 Tunable Filter Made From Three Coupled WGM Resonators
- 22 Dynamic Pupil Masking for Phasing Telescope Mirror Segments

This document was prepared under the sponsorship of the National Aeronautics and Space Administration. Neither the United States Government nor any person acting on behalf of the United States Government assumes any liability resulting from the use of the information contained in this document, or warrants that such use will be free from privately owned rights.



Replaceable Sensor System for Bioreactor Monitoring

An instrument is capable of detecting and monitoring biological media constituents in a spaceflight bioreactor.

Lyndon B. Johnson Space Center, Houston, Texas

A sensor system was proposed that would monitor spaceflight bioreactor parameters. Not only will this technology be invaluable in the space program for which it was developed, it will find applications in medical science and industrial laboratories as well.

Using frequency-domain-based fluorescence lifetime technology, the sensor system will be able to detect changes in fluorescence lifetime quenching that results from displacement of fluorophore-labeled receptors bound to target ligands. This device will be used to monitor and regulate bioreactor parameters including glucose, pH, oxygen pressure (pO_2), and carbon dioxide pressure (pCO_2). Moreover, these biosensor fluorophore receptor-quenching complexes can be designed to further detect and monitor for potential biohazards, bio-products, or bioimpurities.

Biosensors used to detect biological fluid constituents have already been developed that employ a number of strategies, including invasive microelectrodes (e.g., dark electrodes), optical techniques including fluorescence, and membrane permeable systems based on osmotic pressure. Yet the longevity of any of these sensors does not meet the demands of extended use in spacecraft habitat or bioreactor monitoring. It was therefore necessary to develop a sensor platform that could determine not only fluid variables such as glucose concentration, pO_2 , pCO_2 , and pH but can also regulate these fluid variables with controlled feedback loop.

To accommodate the inevitable failure of sensing elements, a biosensor array must be noninvasive and interchangeable — something missing in the current state of the art. Robust, compact, *in-situ* biosensor arrays that are easy to use and self-contained are needed for the on-board testing and monitoring of bioreactor parameters. In a miniaturized frequency-domain lifetime fluorescence (fLF) system, sensor arrays can be integrated into a “dead leg” where the desired assays of bioreactor constituents can be analyzed and results can be sent to a feedback control of regulatory valves that will release nutrients and maintain a constant bioenvironment for cell or tissue culture growth.

The sensor array and dead-leg test solution must be designed so that they are interchangeable for the inevitable requirement of sensor replacement. This design will take into account sterilization considerations as well as the ease with which a part can be replaced in order to minimize the use of astronaut time. The dead leg will allow a small volume of sample to be directed over the fLF sensor surface in order to collect multicomponent emissions and analyze them for different constituents. The biosensor system will also contain feedback controls to the feed lines of the bioreactor, thus providing autonomous operation.

The final fLF sensor system will contain a fully optimized sensor array that can be interfaced with the dead leg of a bioreactor or bioenvironment where current fLF

analysis can be performed repeatedly and then replaced when sensor failure occurs. The fLF has a proven track record and the small dimensions needed to accommodate removable and interchangeable interfacing with the bioreactor/bioenvironment. Scientists believe that an even smaller dimension system can be developed for interfacing directly with the bioreactor. This sensor platform, which will be built around this dead-leg sample analysis segment, will be used for preflight testing/evaluation as a solution to bioreactor environment control and will also be marketed in a development program for use in bioreactor control in the biopharmaceutical and medical industries.

The development of this multi-analyte biosensor system has broad commercial applications in the biopharmaceutical industry where genetically engineered drugs are produced by bioreactors. In addition to its use for bioreactor monitoring, this fLF biosensor technology will be useful for biosensor applications including detection of toxins, dangerous chemicals, and hazardous environmental agents. In addition to monitoring bioreactor parameters during long spaceflights of the future, this system can be used to monitor for biohazards to ensure astronaut safety.

This work was done by Mike Mayo, Steve Savoy, and John Bruno of Systems & Processes Engineering Corporation for Johnson Space Center. For further information, contact the Johnson Technology Transfer Office at (281) 483-3809. MSC-23032.

Unitary Shaft-Angle and Shaft-Speed Sensor Assemblies

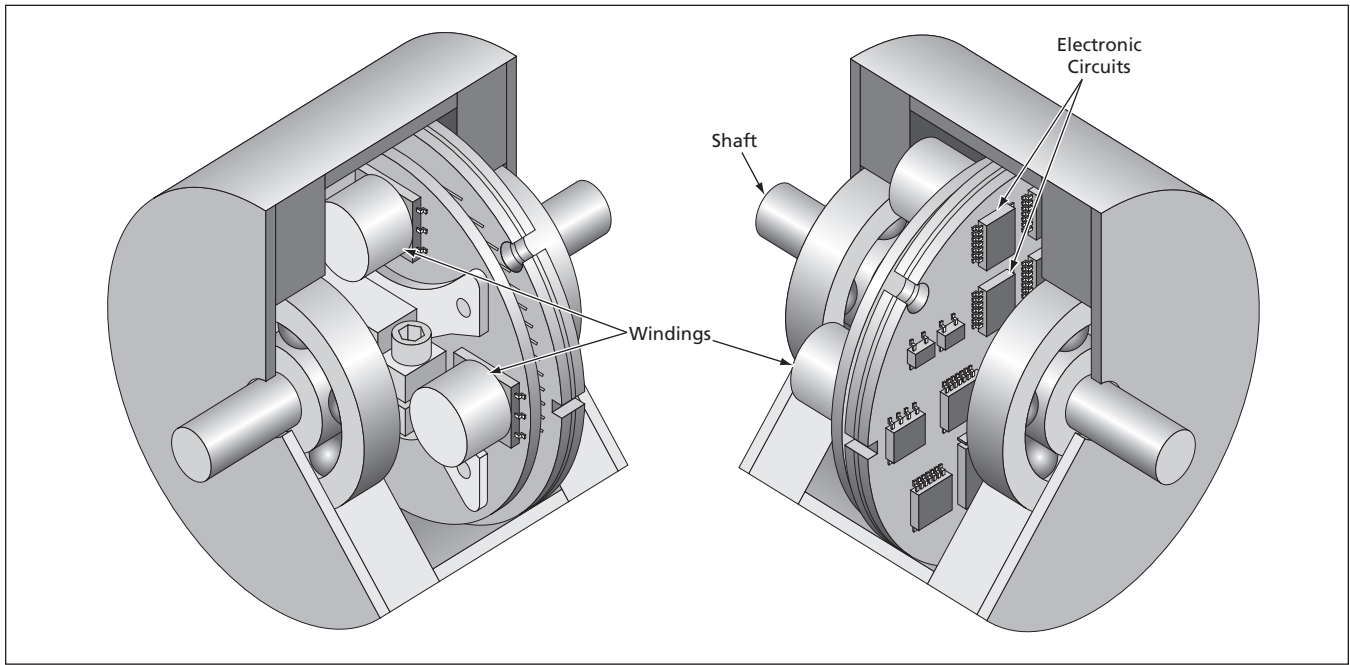
All necessary mechanical and electronic components are packaged together in compact units.

Marshall Space Flight Center, Alabama

The figure depicts a unit that contains a rotary-position or a rotary-speed sensor, plus electronic circuitry necessary for its operation, all enclosed in a single housing with a shaft for coupling to an external rotary machine. This rotation-

sensor unit is complete: when its shaft is mechanically connected to that of the rotary machine and it is supplied with electric power, it generates an output signal directly indicative of the rotary position or speed, without need for addi-

tional processing by other circuitry. The incorporation of all of the necessary excitatory and readout circuitry into the housing (in contradistinction to using externally located excitatory and/or readout circuitry) in a compact arrange-



Transducers and Readout Electronic Circuits are parts of a sensor assembly contained in a single housing.

ment is the major difference between this unit and prior rotation-sensor units.

The sensor assembly inside the housing includes excitatory and readout integrated circuits mounted on a circular printed-circuit board. In a typical case in which the angle or speed transducer(s) utilize electromagnetic induction, the assembly also includes another circular printed-circuit board on which the transducer windings are mounted. A sheet of high-magnetic-permeability metal ("mu metal") is placed between the winding board and

the electronic-circuit board to prevent spurious coupling of excitatory signals from the transducer windings to the readout circuits.

The housing and most of the other mechanical hardware can be common to a variety of different sensor designs. Hence, the unit can be configured to generate any of variety of outputs by changing the interior sensor assembly. For example, the sensor assembly could contain an analog tachometer circuit that generates an output proportional (in both magnitude and

sign or in magnitude only) to the speed of rotation.

This work was done by Dean C. Alhorn, David E. Howard, and Dennis A. Smith of Marshall Space Flight Center. Further information is contained in a TSP (see page 1).

This invention has been patented by NASA (U.S. Patent No. 6,313,624). Inquiries concerning nonexclusive or exclusive license for its commercial development should be addressed to Sammy Nabors, MSFC Commercialization Assistance Lead, at sammy.a.nabors@nasa.gov. Refer to MFS-31238.

Arrays of Nano Tunnel Junctions as Infrared Image Sensors

High detectivity and rapid response would be attainable at room temperature.

NASA's Jet Propulsion Laboratory, Pasadena, California

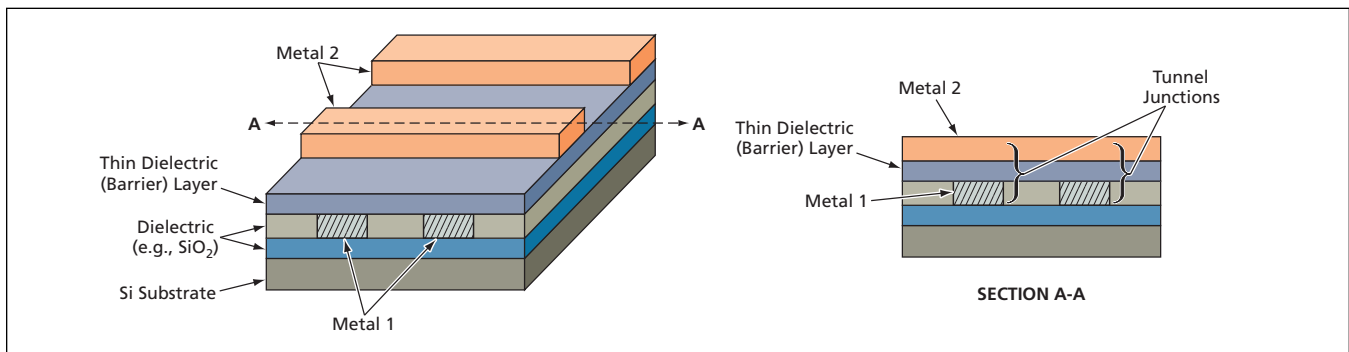
Infrared image sensors based on high-density rectangular planar arrays of nano tunnel junctions have been proposed. These sensors would differ fundamentally from prior infrared sensors based, variously, on bolometry or conventional semiconductor photodetection.

Infrared image sensors based on conventional semiconductor photodetection must typically be cooled to cryogenic temperatures to reduce noise to acceptably low levels. Some bolometer-type infrared sensors can be operated at room temperature, but they exhibit low detectivities and long response

times, which limit their utility. The proposed infrared image sensors could be operated at room temperature without incurring excessive noise, and would exhibit high detectivities and short response times. Other advantages would include low power demand, high resolution, and tailorability of spectral response.

Neither bolometers nor conventional semiconductor photodetectors, the basic detector units as proposed would partly resemble rectennas. Nanometer-scale tunnel junctions would be created by crossing of nanowires with quantum-me-

chanical-barrier layers in the form of thin layers of electrically insulating material between them (see figure). A microscopic dipole antenna sized and shaped to respond maximally in the infrared wavelength range that one seeks to detect would be formed integrally with the nanowires at each junction. An incident signal in that wavelength range would become coupled into the antenna and, through the antenna, to the junction. At the junction, the flow of electrons between the crossing wires would be dominated by quantum-mechanical tunneling rather than thermionic emission. Rela-



Crossed Nanowires with dielectric barriers between them would constitute quantum-mechanical-tunneling junctions that could be used to detect infrared radiation. This device would be fabricated by a process including electron-beam lithography, deposition of metal, and etching. For simplicity, antennas that would be formed integrally with the nanowires are omitted.

tive to thermionic emission, quantum-mechanical tunneling is a fast process. As described below, the quantum-mechanical tunneling would be exploited to rectify the infrared-frequency alternating signal delivered to the junction from the antenna.

Each nanojunction would be asymmetrical in that the crossing nanowires would be made of two different materials: for example, two different metals, a metal and semiconductor, or the same semiconductor doped at two different levels. The resulting asymmetry and nonlinearity of the tunneling current as a function of voltage across the junction could be exploited to effect rectification of the signal. Because the asymmetry

would be present even in the absence of bias, the device could be operated at low or zero bias and, therefore, would demand very little power.

Other advantages of the proposed sensors would include the following:

- High spatial resolution would be achieved by virtue of the density of nanowires and, consequently, of nanojunctions.
- The barriers are expected to keep dark currents very small, leading to high signal-to-noise ratios.
- Different nanojunctions within the same sensor could be fabricated with antennas tailored for different wavelengths, enabling multispectral imaging.

This work was done by Kyung-Ah Son of Caltech; Jeong S. Moon of HRL, LLC; and

Nicholas Prokopuk of Naval Air Warfare Center for NASA's Jet Propulsion Laboratory. Further information is contained in a TSP (see page 1).

In accordance with Public Law 96-517, the contractor has elected to retain title to this invention. Inquiries concerning rights for its commercial use should be addressed to:

*Innovative Technology Assets Management
JPL*

*Mail Stop 202-233
4800 Oak Grove Drive
Pasadena, CA 91109-8099
(818) 354-2240*

E-mail: iaoffice@jpl.nasa.gov

Refer to NPO-42587, volume and number of this NASA Tech Briefs issue, and the page number.

🌀 Catalytic-Metal/PdO_x/SiC Schottky-Diode Gas Sensors

PdO_x layers inhibit the undesired formation of metal silicides.

John H. Glenn Research Center, Cleveland, Ohio

Miniaturized hydrogen- and hydrocarbon-gas sensors, heretofore often consisting of Schottky diodes based on catalytic metal in contact with SiC, can be improved by incorporating palladium oxide (PdO_x, where 0 ≤ x ≤ 1) between the catalytic metal and the SiC.

In prior such sensors in which the catalytic metal was the alloy PdCr, diffusion and the consequent formation of oxides and silicides of Pd and Cr during operation at high temperature were observed to cause loss of sensitivity. However, it was also observed that any PdO_x layers that formed and remained at PdCr/SiC interfaces acted as barriers to diffusion, preventing further deterioration by preventing the subsequent formation of metal silicides.

In the present improvement, the lesson learned from these observations is

applied by placing PdO_x at the catalytic-metal/SiC interfaces in a controlled and uniform manner to form stable diffusion barriers that prevent formation of metal silicides. A major advantage of PdO_x over other candidate diffusion-barrier materials is that PdO_x is a highly stable oxide that can be incorporated into gas-sensor structures by use of deposition techniques that are standard in the semiconductor industry.

The PdO_x layer can be used in a gas sensor structure for improved sensor stability, while maintaining sensitivity. For example, in proof-of-concept experiments, Pt/PdO_x/SiC Schottky-diode gas sensors were fabricated and tested. The fabrication process included controlled sputter deposition of PdO_x to a thickness of ≈50 Å on a 400-μm-thick SiC substrate, followed by deposition of Pt to a

thickness of ≈450 Å on the PdO_x. The SiC substrate (400 microns in thickness) was patterned with photoresist and a Schottky-diode photomask. A lift-off process completed the definition of the Schottky-diode pattern.

The sensors were tested by measuring changes in forward currents at a bias potential of 1 V during exposure to H₂ in N₂ at temperatures ranging from 450 to 600 °C for more than 750 hours. The sensors were found to be stable after a break-in time of nearly 200 hours. The sensors exhibited high sensitivity: sensor currents changed by factors ranging from 300 to 800 when the gas was changed from pure N₂ to 0.5 percent H₂ in N₂. The high sensitivity and stability of these Pt/PdO_x/SiC sensors were found to represent a marked improvement over comparable Pt/SiC sensors. More-

over, surface analysis showed that there was no significant formation of silicides in the Pt/PdO_x/SiC sensors.

*This work was done by Gary W. Hunter and Jennifer C. Xu of **Glenn Research***

Center and Dorothy Lukco of QSS Group, Inc. Further information is contained in a TSP (see page 1).

Inquiries concerning rights for the commercial use of this invention should be addressed

to NASA Glenn Research Center, Innovative Partnerships Office, Attn: Steve Fedor, Mail Stop 4-8, 21000 Brookpark Road, Cleveland, Ohio 44135. Refer to LEW-17859-1.

Compact, Precise Inertial Rotation Sensors for Spacecraft

NASA's Jet Propulsion Laboratory, Pasadena, California

A document describes a concept for an inertial sensor for measuring the rotation of an inertially stable spacecraft around its center of gravity to within 100 microarcseconds or possibly even higher precision. Whereas a current proposal for a spacecraft-rotation sensor of this accuracy requires one spacecraft dimension on the order of ten meters, a sensor according to this proposal could fit within a package smaller than 1 meter and would have less than a tenth of the mass. According to the

concept, an inertial mass and an apparatus for monitoring the mass would be placed at some known distance from the center of gravity so that any rotation of the spacecraft would cause relative motion between the mass and the spacecraft. The relative motion would be measured and, once the displacement of the mass exceeded a prescribed range, a precisely monitored restoring force would be applied to return the mass to a predetermined position. Measurements of the relative mo-

tion and restoring force would provide information on changes in the attitude of the spacecraft. A history of relative motion and restoring-force measurements could be kept, enabling determination of the cumulative change in attitude during the observation time.

*This work was done by David Rosing, Jeffrey Oseas, and Robert Korechoff of Caltech for **NASA's Jet Propulsion Laboratory**. Further information is contained in a TSP (see page 1).
NPO-41926*



Universal Controller for Spacecraft Mechanisms

The controller interfaces to spacecraft sensors and power.

NASA's Jet Propulsion Laboratory, Pasadena, California

An electronic control unit has been fabricated and tested that can be replicated as a universal interface between the electronic infrastructure of a spacecraft and a brushless-motor (or other electromechanical actuator) driven mechanism that performs a specific mechanical function within the overall spacecraft system. The unit includes interfaces to a variety of spacecraft sensors, power outputs, and has selectable actuator control parameters making the assembly a mechanism controller. Several control topologies are selectable and reconfigurable at any time. This allows the same actuator to perform different functions during the mission life of the spacecraft. The unit includes complementary metal oxide/semiconductor electronic components on a circuit board of a type called "rigid flex" (signifying flexible printed wiring along with a rigid sub-

strate). The rigid flex board is folded to make the unit fit into a housing on the back of a motor. The assembly has redundant critical interfaces, allowing the controller to perform time-critical operations when no human interface with the hardware is possible. The controller is designed to function over a wide temperature range without the need for thermal control, including withstanding significant thermal cycling, making it usable in nearly all environments that spacecraft or landers will endure. A prototype has withstood 1,500 thermal cycles between -120 and $+85$ °C without significant deterioration of its packaging or electronic function. Because there is no need for thermal control and the unit is addressed through a serial bus interface, the cabling and other system hardware are substantially reduced in quantity and complexity, with corresponding

reductions in overall spacecraft mass and cost.

This work was done by Greg Levanas, Thomas McCarthy, Don Hunter, Christine Buchanan, Michael Johnson, Raymond Cozy, Albert Morgan, and Hung Tran of Caltech for NASA's Jet Propulsion Laboratory. Further information is contained in a TSP (see page 1).

In accordance with Public Law 96-517, the contractor has elected to retain title to this invention. Inquiries concerning rights for its commercial use should be addressed to:

*Innovative Technology Assets Management
JPL*

Mail Stop 202-233

4800 Oak Grove Drive

Pasadena, CA 91109-8099

(818) 354-2240

E-mail: iaoffice@jpl.nasa.gov

Refer to NPO-41776, volume and number of this NASA Tech Briefs issue, and the page number.

The Flostation — an Immersive Cyberspace System

Neutral buoyancy is exploited along with advanced computer-generated displays.

Lyndon B. Johnson Space Center, Houston, Texas

A flostation is a computer-controlled apparatus that, along with one or more computer(s) and other computer-controlled equipment, is part of an immersive cyberspace system. The system is said to be "immersive" in two senses of the word: (1) It supports the body in a modified form neutral posture experienced in zero gravity and (2) it is equipped with computer-controlled display equipment that helps to give the occupant of the chair a feeling of immersion in an environment that the system is designed to simulate.

Neutral immersion was conceived during the Gemini program as a means of training astronauts for working in a zero-gravity environment. Current derivatives include neutral-buoyancy tanks and the KC-135 airplane, each of which mimics the effects of zero gravity. While these have performed well in simulating the

shorter-duration flights typical of the space program to date, a training device that can take astronauts to the next level will be needed for simulating longer-duration flights such as that of the International Space Station. The flostation is expected to satisfy this need. The flostation could also be adapted and replicated for use in commercial ventures ranging from home entertainment to medical treatment.

The use of neutral immersion in the flostation enables the occupant to recline in an optimal posture of rest and meditation. This posture, combines savasana (known to practitioners of yoga) and a modified form of the neutral posture assumed by astronauts in outer space. As the occupant relaxes, awareness of the physical body is reduced. The neutral body posture, which can be maintained for hours without dis-

comfort, is extended to the eyes, ears, and hands. The occupant can be surrounded with a full-field-of-view visual display and "nearphone" sound, and can be stimulated with full-body vibration and motion cueing. Once fully immersed, the occupant can use neutral hand controllers (that is, hand-posture sensors) to control various aspects of the simulated environment.

A logical extension of the basic flostation concept is the concept of a florum — a system of multiple flostations that can be used by multiple occupants working either by themselves or interaction with each other. As the use of flostations spreads, the immersive cyberspace environments that they create will likely appeal to a vast audience. Indeed, the inventor of the flostation foresees a day when floors will be installed in venues as diverse as hotels, museums, airports, and

theme parks — a far cry from the utilitarian scope of neutral immersion as conceived in the early days of space-flight. Florooms would enable users to share experiences on a large scale — for example, immersive rock concerts or sporting events. A floroom could contain hundreds of flostations.

At present, the flostation is available in two versions. One is a static version, which includes the chair portion (the flochair) equipped with a hemispherical screen (the flodome) that is lowered over the occupant's head so the occupant's eyes are at the center of the dome

and the field of view is filled by an image generated on a standard liquid-crystal-display projector. The static version also includes shakers and loudspeakers mounted on a simple motorized reclining base. The other version is a dynamic one in that the flochair is mounted on a six-degree-of-freedom hydraulic base. The static version is intended for public and home use; the dynamic version is better suited to the space program.

Flostations could prove beneficial in applications beyond the space program for which they were originally developed. For example, they might be used

in medicine for pain-reduction therapy or to treat psychoses.

This work was done by Brian Park of Flogiston Corp. for Johnson Space Center.

In accordance with Public Law 96-517, the contractor has elected to retain title to this invention. Inquiries concerning rights for its commercial use should be addressed to:

*Flogiston Corp.
16921 Crystal Cave Drive
Austin, TX 78737*

Refer to MSC-22932, volume and number of this NASA Tech Briefs issue, and the page number.

Algorithm for Aligning an Array of Receiving Radio Antennas

Relative to prior such algorithms, this one requires less hardware.

NASA's Jet Propulsion Laboratory, Pasadena, California

A digital-signal-processing algorithm (somewhat arbitrarily) called "SUMPLE" has been devised as a means of aligning the outputs of multiple receiving radio antennas in a large array for the purpose of receiving a weak signal transmitted by a single distant source. As used here, "aligning" signifies adjusting the delays and phases of the outputs from the various antennas so that their relatively weak replicas of the desired signal can be added coherently to increase the signal-to-noise ratio (SNR) for improved reception, as though one had a single larger antenna. The method was devised to enhance spacecraft-tracking and telemetry operations in NASA's Deep Space Network (DSN); the method could also be useful in such other applications as both satellite and terrestrial radio communications and radio astronomy.

Heretofore, most commonly, alignment has been effected by a process that involves correlation of signals in pairs. This approach necessitates the use of a large amount of hardware — most notably, the $N(N-1)/2$ correlators needed to process signals from all possible pairs of N antennas. Moreover, because the incoming signals typically have low SNRs, the delay and phase adjustments are poorly determined from the pairwise correlations.

SUMPLE also involves correlations, but the correlations are not performed in pairs. Instead, in a partly iterative process, each signal is appropriately weighted and then correlated with a composite signal equal to the sum of the other signals (see Figure 1). One benefit

of this approach is that only N correlation phase wandering: In some other methods

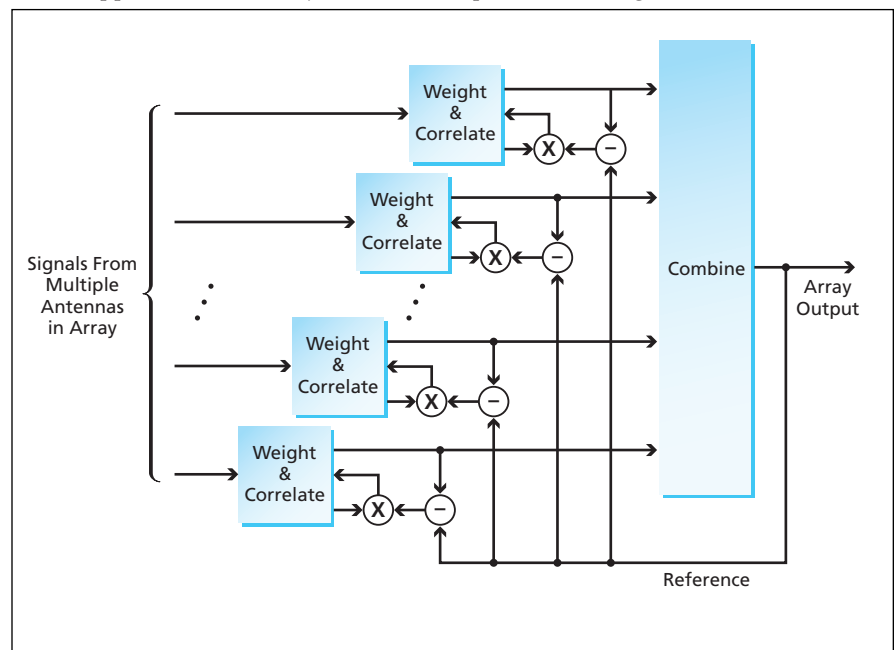


Figure 1. SUMPLE is a digital-signal-processing algorithm in which the signal received by each antenna in an array is correlated with the sum of all the other signals.

tors are needed; in an array of $N \gg 1$ antennas, this results in a significant reduction of the amount of hardware. Another benefit is that once the array achieves coherence, the correlation SNR is $N-1$ times that of a pair of antennas.

Two questions about the performance of SUMPLE have been investigated by computational simulation. The first question is that of how SUMPLE performs at the beginning of a signal-processing pass, before coherence is achieved among the antennas. The second is a question of

of correlation, one antenna is designated the reference antenna and all the other antennas are brought into alignment with it. However, in SUMPLE, all the antennas are aligned to what amounts to a "floating" reference. There is concern as to whether the phase of the floating reference wanders as a function of time, introducing unknown phase instability.

In one simulation, the combining loss as a function of time (equivalently, as a function of the number of iterations) was computed for a 100-antenna array by

use of SUMPLE. At the beginning of the simulated reception process, the signal phases were taken to be random, resulting in a very large combining loss. The

combining loss was found to decrease to a few tenths of a decibel in about eight iterations and to remain at this level thereafter (see Figure 2). Simulations of

many different array configurations yielded essentially the same results.

Answering the question of phase wandering, the simulations did, indeed, show slow phase variations of a few degrees over time intervals of 10 to 20 iterations. However, it was found that this wandering could be prevented by forcing, to zero, the total phase correction obtained by summing the individual corrections over all the antennas. Inasmuch as the phase corrections are meant to bring the antenna signals into alignment with each other, forcing the total phase correction to zero does not pose an obstacle to the achievement of array coherence.

SUMPLE has been tested on an array of 34-m-diameter antennas in the DSN. The results of this test have been found to agree with those of the simulations.

This work was done by David Rogstad of Caltech for NASA's Jet Propulsion Laboratory. Further information is contained in a TSP (see page 1).

The software used in this innovation is available for commercial licensing. Please contact Karina Edmonds of the California Institute of Technology at (818) 393-2827. Refer to NPO-40574.

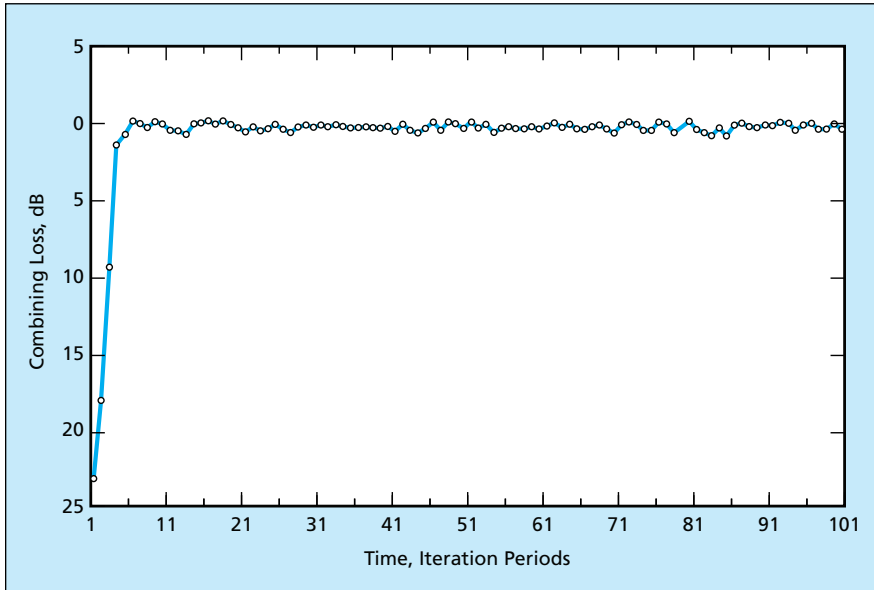


Figure 2. The Combining Loss of a 100-antenna array using SUMPLE was simulated for reception of a representative telemetry signal. The unit of time on the abscissa is an iteration period defined, for the purpose of this specific example, as an integration time of 5,000 telemetry-symbol periods.

Single-Chip T/R Module for 1.2 GHz

T/R modules can be made smaller and at lower cost.

NASA's Jet Propulsion Laboratory, Pasadena, California

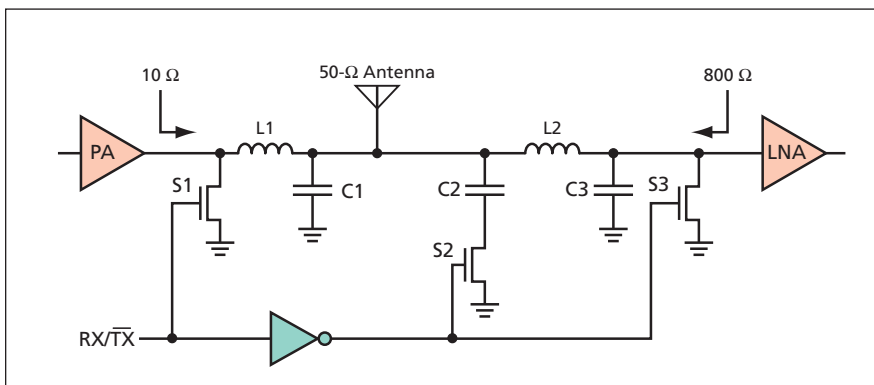
A single-chip CMOS-based (complementary-metal-oxide-semiconductor-based) transmit/receive (T/R) module is being developed for L-band radar systems. Previous T/R module implementations required multiple chips employing different technologies (GaAs, Si, and others) combined with off-chip transmission lines and discrete components including circulators. The new design eliminates the bulky circulator, significantly reducing the size and mass of the T/R module.

Compared to multi-chip designs, the single-chip CMOS can be implemented with lower cost. These innovations enable cost-effective realization of advanced phased array and synthetic aperture radar systems that require integration of thousands of T/R modules.

The circulator is a ferromagnetic device that directs the flow of the RF (radio frequency) power during transmission and reception. During transmission, the circulator delivers the transmitted power from

the amplifier to the antenna, while preventing it from damaging the sensitive receiver circuitry. During reception, the circulator directs the energy from the antenna to the low-noise amplifier (LNA) while isolating the output of the power amplifier (PA). In principle, a circulator could be replaced by series transistors acting as electronic switches. However, in practice, the integration of conventional series transistors into a T/R chip introduces significant losses and noise.

The prototype single-chip T/R module contains integrated transistor switches, but not connected in series; instead, they are connected in a shunt configuration with resonant circuits (see figure). The shunt/resonant circuit topology not only reduces the losses associated with conventional semiconductor switches but also provides beneficial transformation of impedances for the PA and the LNA. It provides full single-pole/double-throw switching for the antenna, isolating the LNA from the transmitted signal and isolating the PA from the received signal. During reception,



A 1.2-GHz Single-Chip T/R Circuit for a radar system eliminates a bulky circulator.

the voltage on control line RX/TX is high, causing the field-effect transistor (FET) switch S1 to be closed, forming a parallel resonant tank circuit L1||C1. This circuit presents high impedance to the left of the antenna, so that the received signal is coupled to the LNA. At the same time, FET switches S2 and S3 are open, so that C2 is removed from the circuit (except for a small parasitic capacitance). The combination of L2 and C3 forms a matching network that transforms the antenna impedance of 50 ohms to a higher value from the perspective of the LNA input terminal. This transformation of impedance improves LNA noise figure by increasing the received voltage delivered to the input transistor. This allows lower transconductance and therefore a smaller transistor, which makes it possible to design the

CMOS LNA for low power consumption. During transmission, the voltage on control line RX/TX is low, causing switch S1 to be open. In this configuration, the combination of L1 and C1 transforms the antenna impedance to a lower value from the perspective of the PA. This low impedance is helpful in producing a relatively high output power compatible with the low CMOS operating potential. At the same time, switches S2 and S3 are closed, forming the parallel resonant tank circuit L2||C2. This circuit presents high impedance to the right of the antenna, directing the PA output signal to the antenna and away from the LNA. During this time, S3 presents a short circuit across the LNA input terminals to guarantee that the voltage seen by the LNA is small enough to prevent damage.

This work was done by Alina Moussessian, Mohammad Mojarradi, Travis Johnson, John Davis, Edwin Grigorian, James Hoffman, and Edward Caro of Caltech; and William Kuhn of Kansas State University for NASA's Jet Propulsion Laboratory. Further information is contained in a TSP (see page 1).

In accordance with Public Law 96-517, the contractor has elected to retain title to this invention. Inquiries concerning rights for its commercial use should be addressed to:

*Innovative Technology Assets Management
JPL*

Mail Stop 202-233

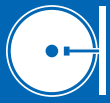
4800 Oak Grove Drive

Pasadena, CA 91109-8099

(818) 354-2240

E-mail: iaoffice@jpl.nasa.gov

Refer to NPO-40869, volume and number of this NASA Tech Briefs issue, and the page number.



Quantum Entanglement Molecular Absorption Spectrum Simulator

Quantum Entanglement Molecular Absorption Spectrum Simulator (QE-MASS) is a computer program for simulating two-photon molecular-absorption spectroscopy using quantum-entangled photons. More specifically, QE-MASS simulates the molecular absorption of two quantum-entangled photons generated by the spontaneous parametric down-conversion (SPDC) of a fixed-frequency photon from a laser. The two-photon absorption process is modeled via a combination of rovibrational and electronic single-photon transitions, using a wave-function formalism. A two-photon absorption cross section as a function of the entanglement delay time between the two photons is computed, then subjected to a fast Fourier transform to produce an energy spectrum. The program then detects peaks in the Fourier spectrum and displays the energy levels of very short-lived intermediate quantum states (or virtual states) of the molecule. Such virtual states were only previously accessible using ultra-fast (femtosecond) laser systems. However, with the use of a single-frequency continuous wave laser to produce SPDC photons, and QE-MASS program, these short-lived molecular states can now be studied using much simpler laser systems. QE-MASS can also show the dependence of the Fourier spectrum on the tuning range of the entanglement time of any externally introduced optical-path delay time. QE-MASS can be extended to any molecule for which an appropriate spectroscopic database is available. It is a means of performing an *a priori* parametric analysis of entangled-photon spectroscopy for development and implementation of emerging quantum-spectroscopic sensing techniques. QE-MASS is currently implemented using the Mathcad® software package.

This program was written by Quang-Viet Nguyen of Glenn Research Center and Jun Kojima of the National Academy of Sciences. Further information is contained in a TSP (see page 1).

Inquiries concerning rights for the commercial use of this invention should be addressed to NASA Glenn Research Center, Innovative Partnerships Office, Attn: Steve Fedor, Mail Stop 4-8, 21000 Brookpark Road, Cleveland, Ohio 44135. Refer to LEW-17830-1.

FuzzObserver

Fuzzy Feature Observation Planner for Small Body Proximity Observations (FuzzObserver) is a developmental computer program, to be used along with other software, for autonomous planning of maneuvers of a spacecraft near an asteroid, comet, or other small astronomical body. Selection of terrain features and estimation of the position of the spacecraft relative to these features is an essential part of such planning. FuzzObserver contributes to the selection and estimation by generating recommendations for spacecraft trajectory adjustments to maintain the spacecraft's ability to observe sufficient terrain features for estimating position. The input to FuzzObserver consists of data from terrain images, including sets of data on features acquired during descent toward, or traversal of, a body of interest. The name of this program reflects its use of fuzzy logic to reason about the terrain features represented by the data and extract corresponding trajectory-adjustment rules. Linguistic fuzzy sets and conditional statements enable fuzzy systems to make decisions based on heuristic rule-based knowledge derived by engineering experts. A major advantage of using fuzzy logic is that it involves simple arithmetic calculations that can be performed rapidly enough to be useful for planning within the short times typically available for spacecraft maneuvers.

This program was written by Ayanna Howard and David Bayard of Caltech for NASA's Jet Propulsion Laboratory. Further information is contained in a TSP (see page 1).

This software is available for commercial licensing. Please contact Karina Edmonds of the California Institute of Technology at (818) 393-2827. Refer to NPO-41290.

Internet Distribution of Spacecraft Telemetry Data

Remote Access Multi-mission Processing and Analysis Ground Environment (RAMPAGE) is a Java-language server computer program that enables near-real-time display of spacecraft telemetry data on any authorized client computer that has access to the Internet and is equipped with Web-browser software. In addition to providing a variety of dis-

plays of the latest available telemetry data, RAMPAGE can deliver notification of an alarm by electronic mail. Subscribers can then use RAMPAGE displays to determine the state of the spacecraft and formulate a response to the alarm, if necessary. A user can query spacecraft mission data in either binary or comma-separated-value format by use of a Web form or a Practical Extraction and Reporting Language (PERL) script to automate the query process. RAMPAGE runs on Linux and Solaris server computers in the Ground Data System (GDS) of NASA's Jet Propulsion Laboratory and includes components designed specifically to make it compatible with legacy GDS software. The client/server architecture of RAMPAGE and the use of the Java programming language make it possible to utilize a variety of competitive server and client computers, thereby also helping to minimize costs.

This program was written by Ted Specht of Caltech and David Noble of Oak Grove Consulting for NASA's Jet Propulsion Laboratory. Further information is contained in a TSP (see page 1).

This software is available for commercial licensing. Please contact Karina Edmonds of the California Institute of Technology at (818) 393-2827. Refer to NPO-41168.

Semi-Automated Identification of Rocks in Images

Rock Identification Toolkit Suite is a computer program that assists users in identifying and characterizing rocks shown in images returned by the Mars Explorer Rover mission. Included in the program are components for automated finding of rocks, interactive adjustments of outlines of rocks, active contouring of rocks, and automated analysis of shapes in two dimensions. The program assists users in evaluating the surface properties of rocks and soil and reports basic properties of rocks. The program requires either the Mac OS X operating system running on a G4 (or more capable) processor or a Linux operating system running on a Pentium (or more capable) processor, plus at least 128MB of random-access memory.

This program was written by Benjamin Bornstein, Andres Castano, and Robert An-

der of Caltech for **NASA's Jet Propulsion Laboratory**. Further information is contained in a TSP (see page 1).

This software is available for commercial licensing. Please contact Karina Edmonds of the California Institute of Technology at (818) 393-2827. Refer to NPO-41133.



Pattern-Recognition Algorithm for Locking Laser Frequency

A computer program serves as part of a feedback control system that locks the frequency of a laser to one of the spectral peaks of cesium atoms in an optical-absorption cell. The system analyzes a saturation absorption spectrum to find a target peak and commands a laser-

frequency-control circuit to minimize an error signal representing the difference between the laser frequency and the target peak. The program implements an algorithm consisting of the following steps:

- Acquire a saturation absorption signal while scanning the laser through the frequency range of interest.
- Condition the signal by use of convolution filtering.
- Detect peaks.
- Match the peaks in the signal to a pattern of known spectral peaks by use of a pattern-recognition algorithm.
- Add missing peaks.
- Tune the laser to the desired peak and thereafter lock onto this peak.

Finding and locking onto the desired peak is a challenging problem, given

that the saturation absorption signal includes noise and other spurious signal components; the problem is further complicated by nonlinearity and shifting of the voltage-to-frequency correspondence. The pattern-recognition algorithm, which is based on Hausdorff distance, is what enables the program to meet these challenges.

This program was written by Vahag Karayan, William Klipstein, Daphna Enzer, Philip Yates, Robert Thompson, and George Wells of Caltech for NASA's Jet Propulsion Laboratory. Further information is contained in a TSP (see page 1).

This software is available for commercial licensing. Please contact Karina Edmonds of the California Institute of Technology at (818) 393-2827. Refer to NPO-41571.



Designing Cure Cycles for Matrix/Fiber Composite Parts

This methodology enables production of void-free laminates.

Langley Research Center, Hampton, Virginia

A methodology has been devised for designing cure cycles to be used in the fabrication of matrix/fiber composite parts (including laminated parts). As used here, "cure cycles" signifies schedules of elevated temperature and pressure as functions of time, chosen to obtain desired rates of chemical conversion of initially chemically reactive matrix materials and to consolidate the matrix and fiber materials into dense solids. Heretofore, cure cycles have been designed following an empirical, trial-and-error approach, which cannot be relied upon to yield optimum results. In contrast, the present methodology makes it possible to design an optimum or nearly optimum cure cycle for a specific application.

Proper design of a cure cycle is critical for achieving consolidation of a reactive-matrix/fiber layup into a void-free laminate. A cure cycle for a composite containing a reactive resin matrix usually consists of a two-stage ramp-and-hold temperature profile. The temperature and the duration of the hold for each stage are unique for a given composite material. The first, lower-temperature ramp-and-hold stage is called the B stage in composite-fabrication terminology. At this stage,

pressure is not applied, and volatiles (solvents and reaction by-products) are free to escape. The second, higher-temperature stage is for final forced consolidation.

The design of such a cure cycle is not trivial. The trial-and-error approach, still commonly used in industry, has several drawbacks:

- Extensive experimentation is usually necessary for determining the proper cure cycle for a given material,
- A cure cycle found to be satisfactory for a given material under one set of conditions may not apply under a different set of conditions, and
- This approach does not ensure that the composite is cured completely under the optimal conditions and shortest amount of time.

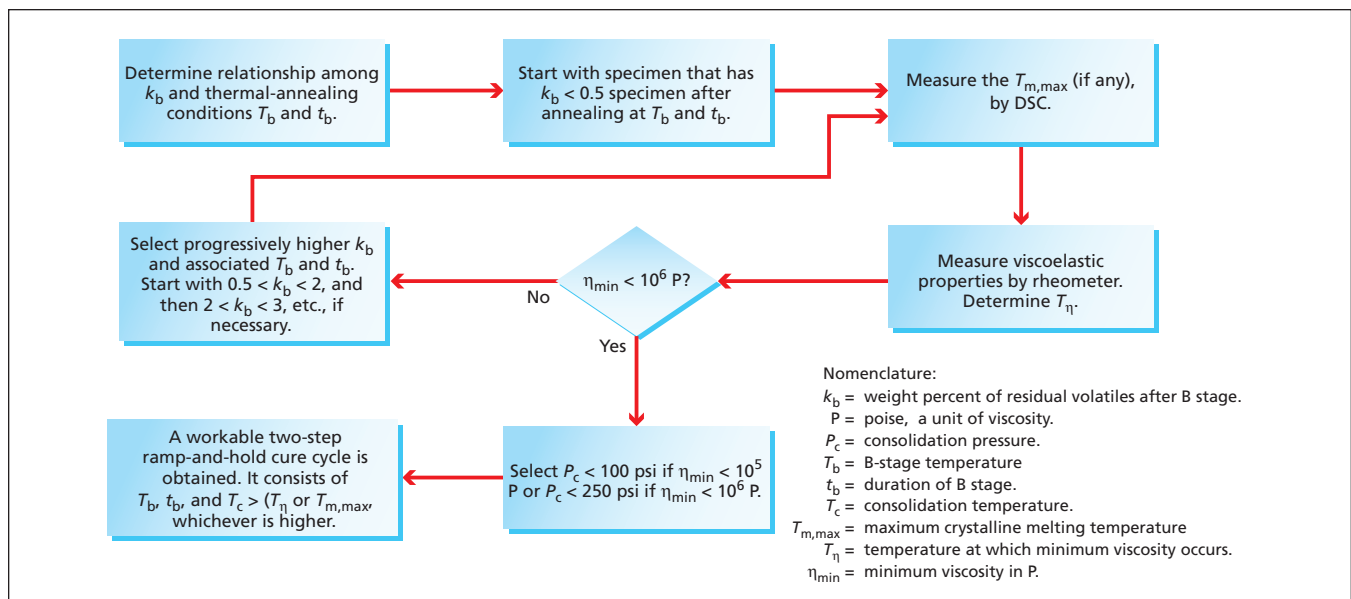
Therefore, the trial-and-error approach is deemed costly, time-consuming, and inefficient as a means of designing cure cycles for the production of laminates of acceptable quality.

In order to make a void-free laminate, one must design the cure cycle to provide for depletion of a sufficient proportion of volatiles through the B stage, before consolidation. However, the viscosity of the resin increases during the

B stage. Therefore, it is necessary to design the B stage so that the residual fluidity of the resin after the B stage is sufficient to enable infiltration of resin through fiber bundles during the subsequent pressure consolidation stage. The problem of balancing between the residual volatile content and the residual fluidity is very complex and unique for a given composite system.

The present methodology is founded on a universal "processing science" approach in which one uses available analytical equipment and techniques to effectively measure and logically analyze and design a workable cycle for any given unique resin/fiber composite. The methodology includes a protocol for:

- Measurements by a thermal gravimetric analyzer (TGA) to characterize mechanisms of depletion of volatiles,
- Differential scanning calorimetry (DSC) to characterize the degrees of imidization reactions and some aspects of the microstructures of partially cured resins, and
- Melt rheometry to characterize the residual fluidity and the temperature of onset of gelation of a partially cured resin.



This Flow Diagram represents the iteration scheme of the cure-cycle-design methodology.

On the basis of these measurements, a workable cure cycle for the subject composite system can be readily and logically designed.

This design methodology involves an iteration scheme (see figure) for satisfying several design criteria to arrive at the design cure cycle for any given thermoset-reactive-matrix-resin/fiber composite system. The number of iterations is based upon scientific judgments instead of empirical reasoning. A workable cure cycle can be established after only one iteration if the following criteria are satisfied:

- The residual volatile content after the B stage is < 0.5 weight percent;
- The forced-consolidation temperature (T_c) exceeds either the maximum crys-

talline melting temperature ($T_{m,max}$) or the temperature at which minimum viscosity occurs (T_η); and

- The residual minimum viscosity (η_{min}) is less than 10^6 poise.

In the event that η_{min} exceeds 10^6 poise, it is necessary to perform a second iteration utilizing a less severe B-stage condition. This condition results in greater fluidity and greater residual volatile content after the B stage. Consequently, η_{min} is reduced to < 10^6 poise, making it possible to use only moderate pressure for final consolidation. Optionally, during the second temperature ramp before final forced consolidation, the application of pressure can be delayed until the temperature reaches T_η in

order to allow for additional depletion of volatiles.

The subject resin/fiber composite material is considered unprocessable (in that a laminated part made of this material cannot be made free of voids) under moderate pressures when the above-mentioned criteria cannot be satisfied concurrently. It is possible to refine the cure cycle by narrowing the B-stage pretreatment conditions in the TGA, DSC, and melt-rheometry analyses.

This work was done by Tan-Hung Hou of Langley Research Center. For further information, contact the Innovative Partnerships Office, NASA Langley Research Center, 3 Langley Boulevard, Mail Stop 200, Hampton, VA 23681-2199. Tel: (757) 864-3936. LAR-16604-1



Controlling Herds of Cooperative Robots

NASA's Jet Propulsion Laboratory, Pasadena, California

A document poses, and suggests a program of research for answering, questions of how to achieve autonomous operation of herds of cooperative robots to be used in exploration and/or colonization of remote planets. In a typical scenario, a flock of mobile sensory robots would be deployed in a previously unexplored region, one of the robots would be designated the leader, and the leader would issue commands to move the robots to different locations or aim sensors at different targets to maximize scientific return. It would be necessary to provide for this hierarchical, cooperative behavior even in the face of such unpredictable factors as terrain obstacles. A potential-fields approach is proposed as

a theoretical basis for developing methods of autonomous command and guidance of a herd. A survival-of-the-fittest approach is suggested as a theoretical basis for selection, mutation, and adaptation of a description of (1) the body, joints, sensors, actuators, and control computer of each robot, and (2) the connectivity of each robot with the rest of the herd, such that the herd could be regarded as consisting of a set of artificial creatures that evolve to adapt to a previously unknown environment. A distributed simulation environment has been developed to test the proposed approaches in the Titan environment. One blimp guides three surface sondes via a potential field approach.

The results of the simulation demonstrate that the method used for control is feasible, even if significant uncertainty exists in the dynamics and environmental models, and that the control architecture provides the autonomy needed to enable surface science data collection.

This work was done by Marco B. Quadrelli of Caltech for NASA's Jet Propulsion Laboratory. For further information, access the Technical Support Package (TSP) free on-line at www.techbriefs.com/tsp under the Software category.

This software is available for commercial licensing. Please contact Karina Edmonds of the California Institute of Technology at (818) 393-2827. Refer to NPO-40723.

Modification of a Limbed Robot to Favor Climbing

A kinematically simplified design affords several benefits.

NASA's Jet Propulsion Laboratory, Pasadena, California

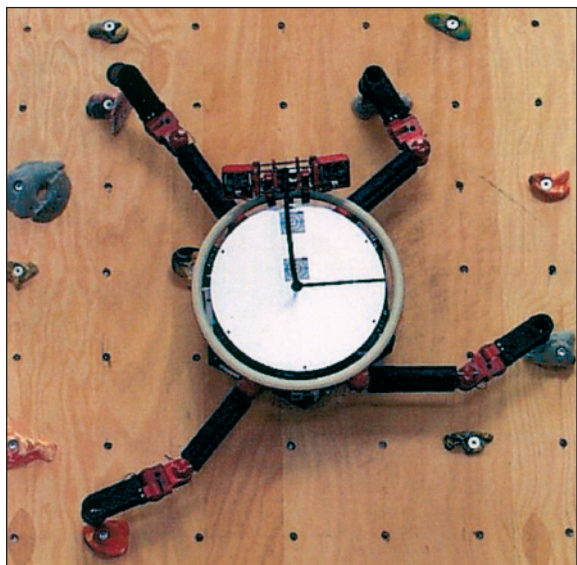
The figure shows the LEMUR I**b**, which is a modified version of the LEMUR II — the second generation of the Limbed Excursion Mechanical Utility Robot (LEMUR). Except as described below, the LEMUR I**b** hard-

ware is mostly the same as that of the LEMUR II. The I**b** and II versions differ in their kinematic configurations and characteristics associated with their kinematic configurations. The differences are such that relative to the LEMUR II, the LEMUR I**b** is simpler and is better suited to climbing on inclined surfaces.

The first-generation LEMUR, now denoted the LEMUR I, was described in "Six-Legged Experimental Robot" (NPO-20897), *NASA Tech Briefs*, Vol. 25, No. 12 (December 2001), page 58. The LEMUR II was described in "Second-Generation Six-Limbed Experimental Robot" (NPO-35140) *NASA Tech Briefs*, Vol. 28, No. 11 (November 2004), page 55. To recapitulate: the LEMUR I and LEMUR II were six-legged or six-

limbed robots for demonstrating robotic capabilities for assembly, maintenance, and inspection. They were designed to be capable of walking autonomously along a truss structure toward a mechanical assembly at a prescribed location. They were equipped with stereoscopic video cameras and image-data-processing circuitry for navigation and mechanical operations. They were also equipped with wireless modems, through which they could be commanded remotely. Upon arrival at a mechanical assembly, the LEMUR I would perform simple mechanical operations by use of one or both of its front legs (or in the case of the LEMUR II, any of its limbs could be used to perform mechanical operations). Either LEMUR could also transmit images to a host computer. The differences between the LEMUR I**b** and the LEMUR II are the following:

- Whereas the LEMUR II had six limbs, the LEMUR I**b** has four limbs. This change has reduced both the complexity and mass of the legs and of the overall robot.



The LEMUR I**b** Walking Robot is simpler and less massive, yet a better climber, relative to its predecessor, the LEMUR II.

- Whereas each limb of the LEMUR II had four degrees of freedom (DOFs), each limb of the LEMUR IIb has three DOFs. This change has also reduced both complexity and mass. Notwithstanding the decrease in the number of DOFs, the three remaining DOFs are configured to provide greater dexterity for motion along a surface.
- To extend reach, the limbs of the LEMUR IIb are 25 percent longer than those of the LEMUR II.
- Additional benefits stemming from the modifications are that the robot body supported by the limbs is now less massive and its center of gravity is now closer to the surface along which the robot is to move.

These benefits have been obtained without sacrificing load-carrying capacity. Hence, overall, the LEMUR IIb is a more adept climber.

This work was done by Avi Okon, Brett Kennedy, Michael Garrett, and Lee Magnone of Caltech for NASA's Jet Propulsion Laboratory. Further information is contained in a TSP (see page 1). NPO-40354



Vacuum-Assisted, Constant-Force Exercise Device

An important advantage over other exercise machines would be light weight.

Lyndon B. Johnson Space Center, Houston, Texas

The vacuum-assisted, constant-force exercise device (VAC-FED) has been proposed to fill a need for a safe, reliable exercise machine that would provide constant loads that could range from 20 to 250 lb (0.09 to 1.12 kN) with strokes that could range from 6 to 36 in. (0.15 to 0.91 m). The VAC-FED was originally intended to enable astronauts in microgravity to simulate the lifting of free weights, but it could just as well be used on Earth for simulated weight lift-

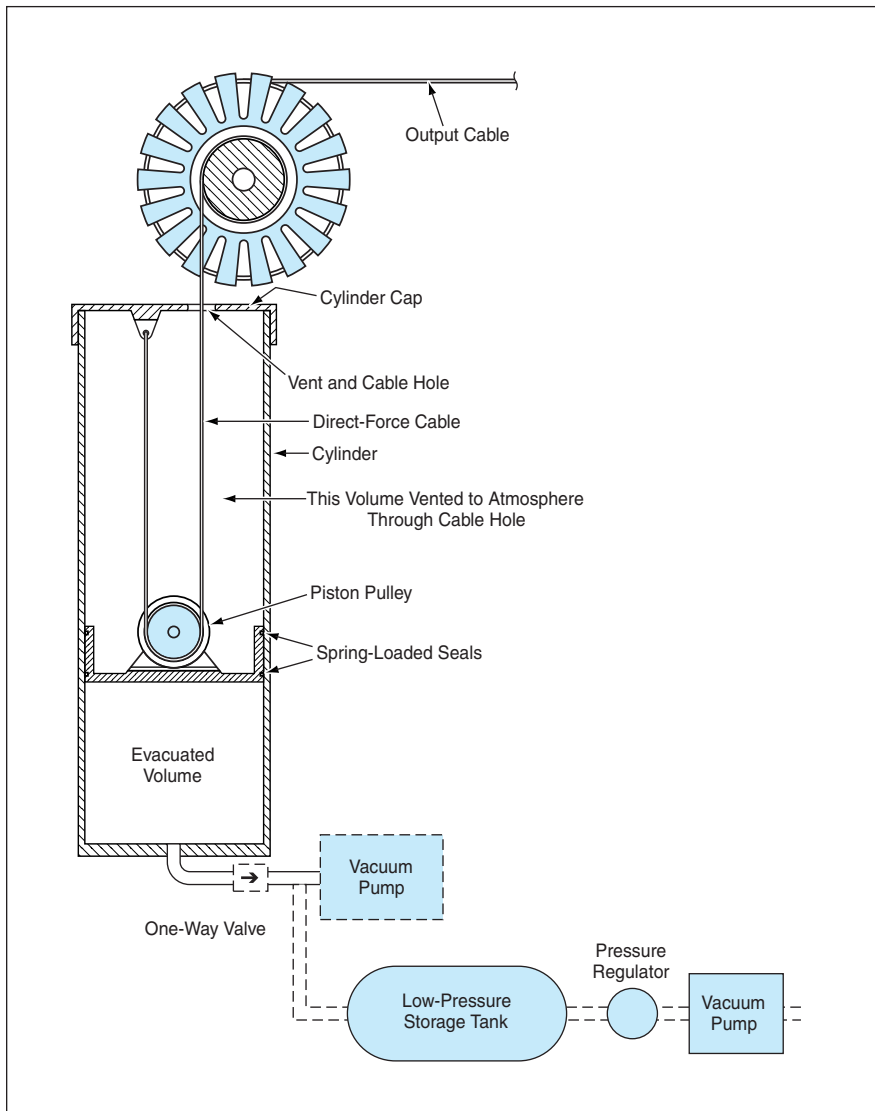
ing and other constant-force exercises. Because the VAC-FED would utilize atmospheric/vacuum differential pressure instead of weights to generate force, it could weigh considerably less than either a set of free weights or a typical conventional exercise machine based on weights. Also, the use of atmospheric/vacuum differential pressure to generate force would render the VAC-FED inherently safer, relative to free weights and to conventional exercise

machines that utilize springs to generate forces.

The overall function of the VAC-FED would be to generate a constant tensile force in an output cable, which would be attached to a bar, handle, or other exercise interface. The primary force generator in the VAC-FED would be a piston in a cylinder. The piston would separate a volume vented to atmosphere at one end of the cylinder from an evacuated volume at the other end of the cylinder (see figure). Hence, neglecting friction at the piston seals, the force generated would be nearly constant — equal to the area of the piston multiplied by the atmospheric/vacuum differential pressure.

In the vented volume in the cylinder, a direct-force cable would be looped around a pulley on the piston, doubling the stroke and halving the tension. One end of the direct-force cable would be anchored to a cylinder cap; the other end of the direct-force cable would be wrapped around a variable-ratio pulley that would couple tension to the output cable. As its name suggests, the variable-ratio pulley would contain a mechanism that could be used to vary the ratio between the tension in the direct-force cable and the tension in the output cable. This mechanism could contain gears, pulleys, and/or levers, for example. By use of this mechanism, the tension in the output cable would be set to a desired fraction of the force generated by the pulley and the stroke would be multiplied by the reciprocal of that fraction.

A vacuum could be generated in several alternative ways. The way that would involve the least equipment would involve the use of a one-way valve in an outlet at the vacuum end of the cylinder (the lower end in the figure). At first, the piston would be forced all the way down in the cylinder to push out most of the air from the lower cylinder volume. Thereafter, the one-way valve would keep air from re-entering the lower cylinder volume, and the device could be used to provide nearly constant tension on the cable during exercise. Of course, air would gradually



Atmospheric/Vacuum Differential Pressure on the piston would be utilized to generate an adjustable, nearly constant tension in the output cable.

leak past the piston seals into the lower cylinder volume, so that it would eventually be necessary to repeat the initial bottoming of the piston to restore the atmospheric/vacuum differential pressure.

Alternatively, a vacuum could be generated and maintained by use of a small manual or electric vacuum

pump. Still another alternative is to connect the lower cylinder volume to the combination of a low-pressure storage tank, pressure regulator, and vacuum pump. This combination could be used to maintain the lower cylinder volume at a subatmospheric pressure (partial vacuum) that could be controlled to set the differential pressure

and thus the output-cable tension at a desired level.

*This work was done by Christopher P. Hansen of **Johnson Space Center** and Scott Jensen of Lockheed Martin Corp. For further information, contact the Johnson Commercial Technology Office at (281) 483-3809.
MSC-23180*

Production of Tuber-Inducing Factor

This substance regulates the growth of potatoes and some other plants.

John F. Kennedy Space Center, Florida

A process for making a substance that regulates the growth of potatoes and some other economically important plants has been developed. The process also yields an economically important by-product: potatoes.

The particular growth-regulating substance, denoted tuber-inducing factor (TIF), is made naturally by, and acts naturally on, potato plants. The primary effects of TIF on potato plants are reducing the lengths of the main shoots, reducing the numbers of nodes on the main stems, reducing the total biomass, accelerating the initiation of potatoes, and increasing the edible fraction (potatoes) of the overall biomass. To some extent, these effects of TIF can override environmental effects that typically inhibit the formation of tubers. TIF can be used in the potato industry to reduce growth time and increase harvest efficiency. Other plants that have been observed to be affected by TIF include tomatoes, peppers, radishes, eggplants, marigolds, and morning glories.

In the present process, potatoes are grown with their roots and stolons immersed in a nutrient solution in a recirculating hydroponic system. From time to time, a nutrient replenishment solution is added to the recirculating nutrient solution to maintain the required

nutrient concentration, water is added to replace water lost from the recirculating solution through transpiration, and an acid or base is added, as needed, to maintain the recirculating solution at a desired pH level. The growing potato plants secrete TIF into the recirculating solution. The concentration of TIF in the solution gradually increases to a range in which the TIF regulates the growth of the plants.

In a procedure for concentrating TIF, no attempt is made to separate TIF from the nutrient and other solutes in the solution. Instead, the solution is simply poured onto flat trays at a depth between 0.5 and 1.0 cm, then concentrated by drying for 12 to 24 hours in a forced-air oven at a temperature of 70 °C. The concentrated solution is stable at and below room temperature and in the presence of ultraviolet light. Optionally, one can freeze-dry the solution to remove all the water, leaving a water-soluble dry powder. The concentrated solution or dry powder is stored in a dry environment. Thereafter, one simply adds deionized water to the concentrated solution or dry powder to make a TIF-containing nutrient solution having the desired lesser concentration.

Results of laboratory tests suggest that TIF-containing solutions made in

this way are suitable for use in diverse settings, including fields, green houses, and enclosed environments containing natural- and artificial-soil-based as well as hydroponic plant-growth systems. Potential commercial applications include the following:

- Hydroponic, aeroponic, or field production of seed potatoes;
- Dwarfing of bedding plants in controlled environments;
- Dwarfing of ornamental plants in fields and in controlled environments; and
- As a quasi-natural regulator (in this case, as a suppressor) of the growth of weeds.

*This work was done by Gary W. Stutte and Neil C. Yorio of Dynamac Corp. for **Kennedy Space Center**.*

Title to this invention, covered by U.S. Patent No. 5,992,090 has been waived under the provisions of the National Aeronautics and Space Act (42 U.S.C. 2457 (f)). Inquiries concerning licenses for its commercial development should be addressed to:

*Gary W. Stutte, Ph.D. or Neil C. Yorio
Phone Nos.: (321) 861-3493 or
(321) 861-2497*

*E-mail: Gary.Stutte-1@ksc.nasa.gov or
Neil.Yorio-1@ksc.nasa.gov*

Refer to KSC-12007/513, volume and number of this NASA Tech Briefs issue, and the page number.



Quantum-Dot Laser for Wavelengths of 1.8 to 2.3 μm

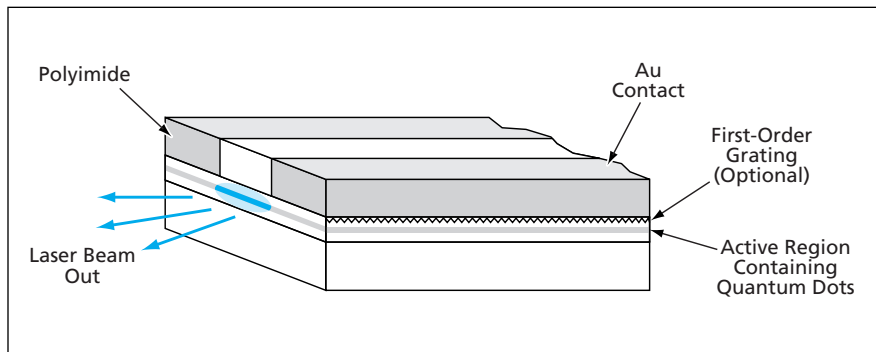
Process conditions must be controlled to form quantum dots at sufficient density.

NASA's Jet Propulsion Laboratory, Pasadena, California

The figure depicts a proposed semiconductor laser, based on In(As)Sb quantum dots on a (001) InP substrate, that would operate in the wavelength range between 1.8 and 2.3 μm . InSb and InAsSb are the smallest-bandgap conventional III-V semiconductor materials, and the present proposal is an attempt to exploit the small bandgaps by using InSb and InAsSb nanostructures as mid-infrared emitters.

The most closely related prior III-V semiconductor lasers are based, variously, on strained InGaAs quantum wells and InAs quantum dots on InP substrates. The emission wavelengths of these prior devices are limited to about 2.1 μm because of critical quantum-well thickness limitations for these lattice-mismatched material systems.

The major obstacle to realizing the proposed laser is the difficulty of fabricating InSb quantum dots in sufficient density on an InP substrate. This difficulty arises partly because of the weakness of the bond between In and Sb and partly because of the high temperature needed to crack metalorganic precursor compounds during the vapor-phase epitaxy used to grow quantum dots: The mobility of the weakly bound In at the high growth temperature is so high that In adatoms migrate easily on the growth surface, resulting in the formation of large InSb islands at a density, usually



In the Proposed Semiconductor Laser, the active region would contain In(As)Sb quantum dots, which emit at wavelengths from 1.7 to 2.3 μm . The first-order grating would be included, optionally, to select operation at a single wavelength.

less than $5 \times 10^9 \text{ cm}^{-2}$, that is too low for laser operation.

The mobility of the In adatoms could be reduced by introducing As atoms to the growth surface because the In-As bond is about 30 percent stronger than is the In-Sb bond. The fabrication of the proposed laser would include a recently demonstrated process that involves the use of alternative supplies of precursors to separate group-III and group-V species to establish local non-equilibrium process conditions, so that In(As)Sb quantum dots assemble themselves on a (001) InP substrate at a density as high as $4 \times 10^{10} \text{ cm}^{-2}$. Room-temperature photoluminescence spectra of quantum dots formed by this process indicate that they emit at wavelengths from 1.7 to 2.3 μm .

This work was done by Yueming Qiu of Caltech for NASA's Jet Propulsion Laboratory. Further information is contained in a TSP (see page 1).

In accordance with Public Law 96-517, the contractor has elected to retain title to this invention. Inquiries concerning rights for its commercial use should be addressed to:

*Innovative Technology Assets Management
JPL*

*Mail Stop 202-233
4800 Oak Grove Drive
Pasadena, CA 91109-8099
(818) 354-2240*

E-mail: iaoffice@jpl.nasa.gov

Refer to NPO-40653, volume and number of this NASA Tech Briefs issue, and the page number.

Tunable Filter Made From Three Coupled WGM Resonators

This is a prototype of high-performance filters for photonic applications.

NASA's Jet Propulsion Laboratory, Pasadena, California

A tunable third-order band-pass optical filter has been constructed as an assembly of three coupled, tunable, whispering-gallery-mode resonators similar to the one described in "Whispering-Gallery-Mode Tunable Narrow-Band-Pass Filter" (NPO-30896), *NASA Tech Briefs*, Vol. 28, No. 4 (April 2004), page 5a. This filter offers a combination of four characteristics that are desirable for

potential applications in photonics: (1) wide real-time tunability accompanied by a high-order filter function, (2) narrowness of the passband, (3) relatively low loss between input and output coupling optical fibers, and (4) a sparse spectrum. In contrast, prior tunable band-pass optical filters have exhibited, at most, two of these four characteristics.

As described in several prior *NASA Tech*

Briefs articles, a whispering-gallery-mode (WGM) resonator is a spheroidal, disklike, or toroidal body made of a highly transparent material. It is so named because it is designed to exploit whispering-gallery electromagnetic modes, which are waveguide modes that propagate circumferentially and are concentrated in a narrow toroidal region centered on the equatorial plane and located near the outermost edge.

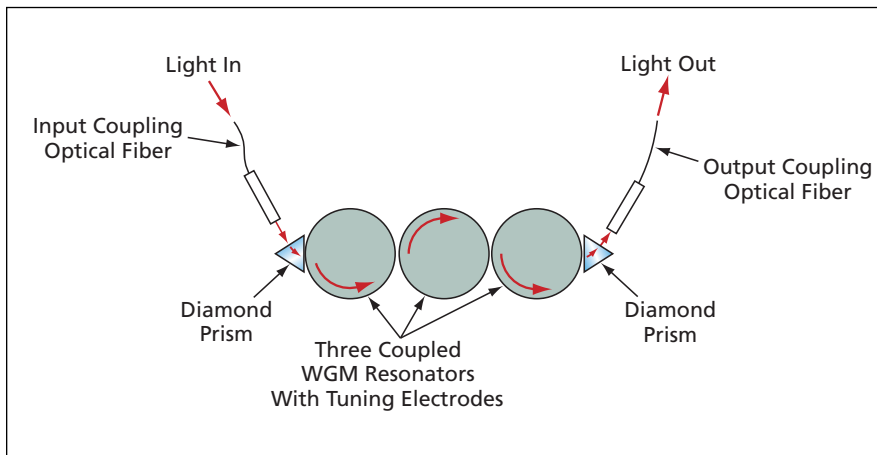


Figure 1. **Three Coupled, Tunable WGM Resonators** constitute a third-order tunable band-pass optical filter.

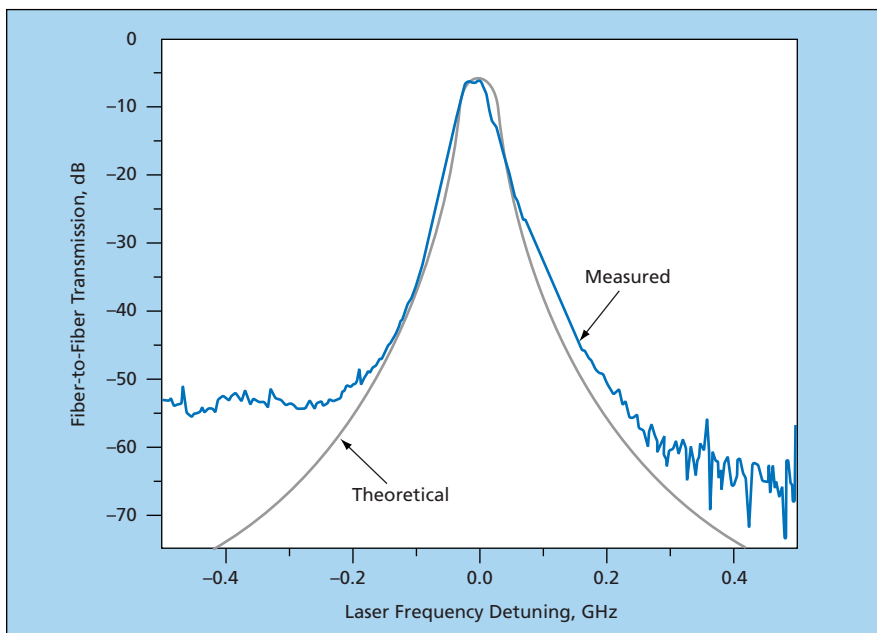


Figure 2. The **Measured Transmission Spectrum** of the filter was fitted with a Butterworth profile function $\gamma^6/[(\nu)^6 + \gamma^6]$, where $\gamma = 29$ MHz and ν is the laser frequency detuning (the difference between the laser frequency and the peak-transmission frequency).

Figure 1 depicts the optical layout of the present filter comprising an assembly of three coupled, tunable WGM resonators. Each WGM resonator is made from a disk of Z-cut LiNbO₃ of 3.3-mm di-

ameter and 50- μ m thickness. The perimeter of the disk is polished and rounded to a radius of curvature of 40 μ m. The free spectral range of each WGM resonator is about 13.3 GHz. Gold coats on the flat

faces of the disk serve as electrodes for exploiting the electro-optical effect in LiNbO₃ for tuning. There is no metal coat on the rounded perimeter region, where the whispering-gallery modes propagate. Light is coupled from an input optical fiber into the whispering-gallery modes of the first WGM resonator by means of a diamond prism. Another diamond prism is used to couple light from the whispering-gallery modes of the third WGM resonator to an output optical fiber.

The filter operates at a nominal wavelength of 1,550 nm and can be tuned over a frequency range of ± 12 GHz by applying a potential in the range of ± 150 V to the electrodes. The insertion loss (the loss between the input and output coupling optical fibers) was found to be repeatable at 6 dB. The resonance quality factor (Q) of the main sequence of resonator modes was found to be 5×10^6 , which corresponds to a bandwidth of 30 MHz. The filter can be shifted from one operating frequency to another within a tuning time ≤ 30 μ s. The transmission curve of the filter at frequencies near the middle of the passband closely approximates a theoretical third-order Butterworth filter profile, as shown in Figure 2.

This work was done by Anatoliy Savchenkov, Vladimir Ilchenko, Lute Maleki, and Andrey Matsko of Caltech for NASA's Jet Propulsion Laboratory. Further information is contained in a TSP (see page 1).

In accordance with Public Law 96-517, the contractor has elected to retain title to this invention. Inquiries concerning rights for its commercial use should be addressed to:

*Innovative Technology Assets Management
JPL*

*Mail Stop 202-233
4800 Oak Grove Drive
Pasadena, CA 91109-8099
(818) 354-2240*

E-mail: iaoffice@jpl.nasa.gov

Refer to NPO-40873, volume and number of this NASA Tech Briefs issue, and the page number.

Dynamic Pupil Masking for Phasing Telescope Mirror Segments

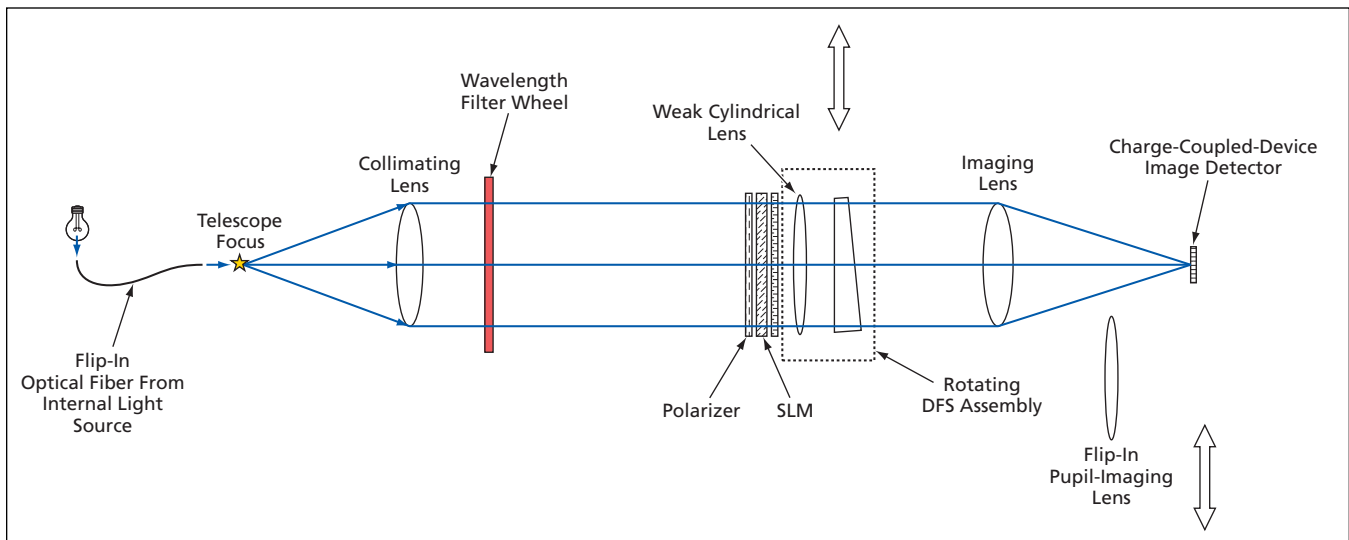
Piston and tilt adjustments could be performed more efficiently.

NASA's Jet Propulsion Laboratory, Pasadena, California

A method that would notably include dynamic pupil masking has been proposed as an enhanced version of a prior method of phasing the segments of a primary telescope mirror. The method

would apply, more specifically, to a primary telescope mirror that comprises multiple segments mounted on actuators that can be used to tilt the segments and translate them along the nominal

optical axis to affect wavefront control in increments as fine as a fraction of a wavelength of light. An apparatus (see figure) for implementing the proposed method would be denoted a dispersed-



A DPCS would combine several telescope-alignment instruments into one that would function more efficiently.

fringe-sensor phasing camera system (DPCS).

The prior method involves the use of a dispersed-fringe sensor (DFS). The prior method was reported as part of a more comprehensive method in “Coarse Alignment of a Segmented Telescope Mirror” (NPO-20770), *NASA Tech Briefs*, Vol. 25, No. 4 (April 2001), page 15a. The pertinent parts of the prior method are the following:

- The telescope would be aimed at a bright distant point source of light (e.g., a star) and form a broadband image on an imaging detector array placed at the telescope focal plane.
- The construction and use of a dispersed-fringe sensor would begin with insertion of a grism (a right-angle prism with a transmission grating on the hypotenuse face) into the optical path. With other segments tilted away from the investigating region of the detector, a dispersed-fringe image would be formed by use of a designated reference segment and a selected mirror segment. The modulation period and orientation of the fringe would be analyzed to determine the magnitude and sign of the piston error (displacement along the nominal optical axis) between the two segments. The error would be used to perform a coarse-phase piston adjustment of the affected mirror segment. This determination and removing of piston

error is what is meant by “phasing” as used above. The procedure as described thus far would be repeated until all segments had been phased.

A major drawback of the prior method is the time-consuming nature of the repeated tilting of mirror segments, necessitated by the fact that the DFS as described above could not be used to phase more than two mirror segments at a time. To be able to phase more than two segments simultaneously, it would be necessary to augment the DFS with an array of prisms and a pupil mask and to implement a complicated pupil-registration process.

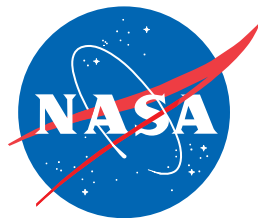
In the proposed method, the need for repeated tilting would be eliminated by using a programmable spatial light modulator (SLM) as a dynamic segment edge mask in conjunction with a weak cylindrical lens: At a given instant of time, the SLM would be made transparent only in areas containing the edges of the mirror segments to be phased. Elsewhere, the SLM would be opaque to block light from all other mirror segments. The SLM would also enable accurate *in situ* pupil registration and could readily be adapted to different segment geometries. Also as part of the proposed method, the weak cylindrical lens would be used to separate DFS fringes across the wavelength dispersion of the grism, thereby making it possible to phase multiple pairs of mirror segments in one image exposure. Hence,

the combination of the SLM and the weak cylindrical lens would greatly increase the efficiency of the segment-phasing process.

Other elements of the proposed method are the following:

- The DPCS could be designed to enable simultaneous measurements on two edge orientations of the hexagonal segments by use of both polarization channels. Alternatively, as shown in the figure, the DFS assembly in the DPCS could be designed to rotate about the optical axis, enabling measurements on all segment edges.
- The combination of a flip-in pupil imaging lens and the SLM would enable accurate pupil registration.
- The DFS assembly could be removed and a weak spherical lens used in combination with the SLM to form a Shack-Hartmann sensor for measuring tilts of mirror segments. In this case, the SLM would be used to create subapertures within each segment.
- The weak spherical lens could also serve as part of a prescription-retrieval sensor, the use of which would enable further reduction of piston errors. In this case, the SLM would be used to form subapertures on the segment edges.

This work was done by Fang Shi, David Redding, Catherine Ohara, and Mitchell Troy of Caltech for NASA’s Jet Propulsion Laboratory. Further information is contained in a TSP (see page 1). NPO-41996



National Aeronautics and
Space Administration